Nuclear Physics B287 (1987) 601–620
North-Holland, Amsterdam

# ON THE RADIATIVE BHABHA SCATTERING FOR THE SINGLE PHOTON CONFIGURATION

C. MANA[1] and M. MARTINEZ[2]

*Deutsches Elektronen-Synchrotron, DESY, Hamburg, Fed. Rep. Germany*

Received 14 July 1986

We present an exact calculation of the process $e^+e^- \to e^+e^-\gamma$ to order $g^3$, that is, including the $\gamma$ and $Z^0$ intermediate vector bosons and keeping fermion masses. This condition is needed to study the contribution of this process as background to single photon events. The calculation has been done at the amplitude level and the strong peaks occurring in the matrix element squared for the single photon configuration have been absorbed by an adequate mapping of the phase space variables. These two facts are necessary in order to obtain a numerically stable integration and an efficient Monte Carlo generator.

## 1. Introduction

The study of single $\gamma$ events in $e^+e^-$ interactions above the $Z^0$ has been proposed a long time ago as a direct method for counting the number of light neutrino types [1]. More recently, the analysis of isolated photons in $e^+e^-$ interactions has been suggested [2] as a clear signature for the existence of supersymmetry particles (like photinos or s-neutrinos) or stable neutral heavy leptons. It is therefore important to have reliable calculations of the background. In this paper, we have studied the radiative Bhabha scattering $e^+e^- \to e^+e^-\gamma$ because, although the transverse momentum of the photon is limited due to the kinematical conditions of antitagging in the final state leptons, the experimental resolution and detection gaps together with the huge cross section of the process represent by far the most important sources of contamination.

The particular kinematical conditions for the observation of an isolated photon make the existing calculations of $e^+e^- \to e^+e^-\gamma$ [3] highly inefficient. On the other hand, to have a reliable calculation for energies of $\sqrt{s} \sim M_{Z^0}$ one has to take into account the width of the $Z^0$ boson and, in order to avoid collinear divergences and to achieve a good stability for the huge cancellations occurring in the evaluation of

[1] On leave of absence from JEN, Madrid, Spain.
[2] On leave of absence from Laboratori de Física d' Altes Energies, Bellaterra, Barcelona, Spain.

0550-3213/87/$03.50 

the matrix element one cannot neglect, at least for some region of the phase space, the fermion masses.

In this paper, we present an exact calculation to order $g^3$ of the process $e^+e^- \to e^+e^-\gamma$, that is, without neglecting the $Z^0$ width and keeping the fermion masses. Moreover, with a detailed study of the phase space we can absorb the peaks in the matrix element through a transformation of variables obtaining a stable integration and a very efficient generation of events. The extension of this calculation to the process $e^+e^- \to f^+f^-\gamma$, models with more intermediate vector bosons and polarized beams is straightforward.

The outline of the paper is as follows. In sect. 2 we explain the technique used for the evaluation of the matrix element. Sect. 3 contains a detailed study of the phase space, the transformations used for the generation of events and the integration of the cross section. In sect. 4 we discuss the results obtained for a reasonable set of experimental conditions. Sect. 5 contains a comparison with other calculations and some remarks on the numerical stability. Last, we present in sect. 6 the conclusions of the analysis. Some interesting details concerning the evaluation of the amplitudes and the phase space are included respectively in appendices A and B.

## 2. The matrix element

Since we are interested in the experimental set-up where the outgoing electron and positron are undetected, we shall keep the fermion masses to avoid collinear divergences. Moreover, we shall keep the width of the $Z^0$ boson so the result will be valid for $\sqrt{s} \sim M_{Z^0}$. With these conditions, it would be rather lengthy to do the calculation by the standard technique of traces reduction. Therefore, we will use the interesting approach of refs. [4–7] and work at the amplitude level (i.e. with complex numbers). This procedure, besides simplifying enormously the calculation, provides a higher numerical accuracy than the traditional method because the huge cancellations between the Feynman diagrams of a gauge invariant subset now take place at the amplitude level.

In order $g^3$, the process

$$e^-(p_1) + e^+(p_2) \to e^-(p_3) + e^+(p_4) + \gamma(k) \tag{1}$$

is represented by the 16 Feynman diagrams shown in fig. 1. If we define the couplings to the photon and the $Z^0$ as

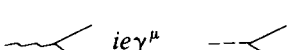


(2a)

where

$$C_L = \frac{-1 + 2\sin^2\vartheta_w}{\sin 2\vartheta_w}, \qquad C_R = \frac{2\sin^2\vartheta_w}{\sin 2\vartheta_w}, \tag{2b}$$

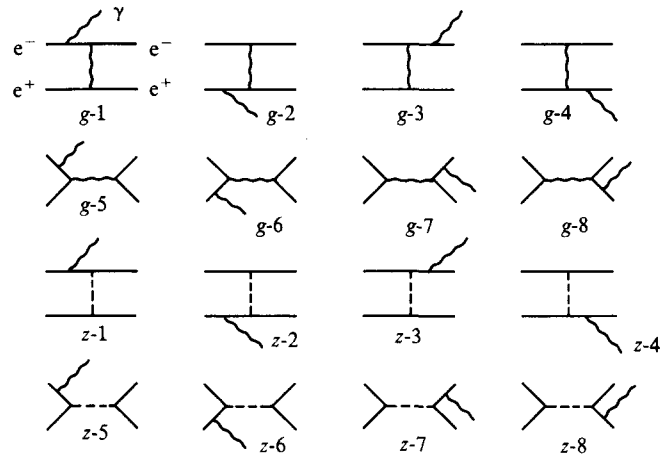


Fig. 1. Feynman diagrams contributing to $e^+e^- \to e^+e^-\gamma$ to order $g^3$.

being $P_L$ ($P_R$) the left- (right-) chirality projectors, and the kinematic invariants

$$s = (p_1 + p_2)^2, \qquad t = (p_1 - p_3)^2, \qquad u = (p_1 - p_4)^2,$$

$$s' = (p_3 + p_4)^2, \qquad t' = (p_2 - p_4)^2, \qquad u' = (p_2 - p_3)^2, \tag{3a}$$

with the relation

$$s + s' + t + t' + u + u' = 4m_e^2 + 4m_f^2, \tag{3b}$$

we can write the amplitude for the diagrams $g$-1 or $z$-1 as

$$iM_1 = \frac{ie^3}{2(p_1k)F(t)} T_1(p_i, \lambda_i), \tag{4a}$$

where

$$T_1(p_i, \lambda_i) = [\bar{u}(p_3, \lambda_3)\Gamma^\mu(\not{p}_1 - \not{k} + m)\not{\epsilon}^*(k, \lambda_k)u(p_1, \lambda_1)] \times [\bar{v}(p_2, \lambda_2)\Gamma_\mu v(p_4, \lambda_4)] \tag{4b}$$

and

$$\Gamma^\mu = \begin{cases} \gamma^\mu, & \text{for the photon} \\ \gamma^\mu(C_L P_L + C_R P_R), & \text{for the } Z^0 \end{cases}, \tag{4c}$$

$$F(y) = \begin{cases} y, & \text{for the photon} \\ (y - M_{Z^0}^2) + iM_{Z^0}\Gamma_{Z^0}, & \text{for the } Z^0 \end{cases} \tag{4d}$$

The amplitudes for the remaining diagrams can be directly obtained from this one by the appropriate permutation of variables and conjugations. Therefore, we shall deal from now on only with $iM_1$ given by the eqs. (4).

Once we have the expression (4b) we can assume that, for calculational purposes, antiparticles have a negative mass and introduce the relation

$$\sum_{\lambda} u(p,\lambda)\bar{u}(p,\lambda) = \not{p} + m, \tag{5}$$

treating the spinors $u(p,\lambda)$ and $v(p,\lambda)$ in the same way. Moreover, if we consider that any $\not{p}$ corresponding to a massless particle represented by $u(p,\lambda)$ can be expressed as

$$\sum_{\lambda} u(p,\lambda)\bar{u}(p,\lambda) = \not{p}, \tag{6}$$

we can formally rewrite the expression (4b) as

$$T_1(p_i,\lambda_i) = \sum_{\lambda} \big[\bar{u}(p_3,\lambda_3)\Gamma^{\mu}(u(p_1,\lambda)\bar{u}(p_1,\lambda) - u(k,\lambda)\bar{u}(k,\lambda))\not{\epsilon}^{*}(k,\lambda_k)u(p_1,\lambda_1)\big] \times \big[\bar{u}(p_2,\lambda_2)\Gamma_{\mu}u(p_4,\lambda_4)\big]. \tag{7}$$

Following ref. [6] we can express the spinors $u(p_i,\lambda_i)$ in terms of the more elementary chiral ones $w(p_i,\lambda_i)$ like

$$u(p_i,\lambda_i) = w(p_i,\lambda_i) + \mu_i w(k_0,-\lambda_i), \tag{8a}$$

where $\mu_i = m_i/\eta_i$, $\eta_i = \sqrt{2(p_i\cdot k_0)}$ and

$$w(p_i,\lambda_i) = \not{p}_i w(k_0,-\lambda_i)/\eta_i \tag{8b}$$

being the spinors $w(k_0,\lambda)$ chosen such that

$$w(k_0,\lambda)\bar{w}(k_0,\lambda) = \frac{1+\lambda\gamma^5}{2}\not{k}_0 \tag{8c}$$

and

$$w(k_0,\lambda) = \lambda \not{k}_1 w(k_0,-\lambda), \tag{8d}$$

with $k_0^\mu$ and $k_1^\mu$ any four-vectors (here taken to be $k_0^\mu = (1,1,0,0)$ and $k_1^\mu = (0,0,1,0)$) different from $p_i$ $(i = 1,4)$ and $k$ and satisfying

$$k_0^\mu k_{\mu 0} = k_0^\mu k_{1\mu} = 0, \qquad k_1^\mu k_{1\mu} = -1. \tag{9}$$

It is important to point out that the spinors $w(p_i, \lambda_i)$ and $w(k_0, -\lambda_i)$ are quite different. One has therefore to be aware of whether the four-momentum variable is $p_i^\mu$ or $k_0^\mu$.

Once we have these definitions, we can express the product of two bilinears

$$Z(p_i, \lambda_i; p_j, \lambda_j; p_k, \lambda_k; p_l, \lambda_l) \equiv \left[\bar{u}(p_i, \lambda_i)\Gamma^\mu u(p_j, \lambda_j)\right]\left[\bar{u}(p_k, \lambda_k)\Gamma'_\mu u(p_l, \lambda_l)\right] \tag{10}$$

in terms of the spinors $w(p, \lambda)$ for which we introduce*

$$\tilde{Z}(q_i, \lambda_i; q_j, \lambda_j; q_k, \lambda_k; q_l, \lambda_l) \equiv \left[\bar{w}(q_i, \lambda_i)\gamma^\mu w(q_j, \lambda_j)\right]\left[\bar{w}(q_k, \lambda_k)\gamma_\mu w(q_l, \lambda_l)\right]$$

$$= F^\mu(\lambda_i, q_i, q_j) F_\mu(\lambda_k, q_k, q_l), \tag{11a}$$

where

$$F^\mu(\lambda, q_i, q_j) = \left[\bar{w}(q_i, \lambda)\gamma^\mu w(q_j, \lambda)\right]. \tag{11b}$$

It is a lengthy but straightforward task to demonstrate that the evaluation of the functions $\tilde{Z}(q_i, \lambda_i; q_j, \lambda_j; q_k, \lambda_k; q_l, \lambda_l)$ can be easily performed if, at the level of the functions $F^\mu(\lambda, q_i, q_j)$, we make explicit the difference between $w(p_i, \lambda)$ and $w(k_0, \lambda)$ by using, in all the occurrences, the substitution rule

$$F^\mu(\lambda, k_0, q_j) = -f^\mu(-\lambda, q_j, k_0),$$

$$F^\mu(\lambda, p_i, q_j) = +f^\mu(\lambda, p_i, q_j). \tag{12}$$

After having used explicitly the substitution (12) in the amplitude, we can apply the index elimination property (regardless whether $p_i = k_0$ or not)

$$f^\mu(\lambda, q_i, q_j) f_\mu(\lambda', q_k, q_l) = -2\delta_{\lambda,\lambda'}\mathrm{SM}(\lambda, q_i, q_k)\mathrm{SM}(-\lambda, q_j, q_l)$$

$$-2\delta_{\lambda,-\lambda'}\mathrm{SM}(\lambda, q_i, q_l)\mathrm{SM}(-\lambda, q_j, q_k). \tag{13}$$

* We shall use $p_i$ to denote any four-momenta occurring in the process and $q_i$ to denote any four-vector ($p_i$ or $k_0$).

The quantities $\mathrm{SM}(\lambda, q_i, q_j)$ are just $c$-numbers depending on the components of the four-vectors and are defined in the following way:

(i) For any four-momenta occurring in the process

$$\mathrm{SM}(\lambda, p_i, p_j) \equiv \bar{u}(p_i, \lambda) u(p_j, -\lambda)$$

$$= \lambda \left( (p_i^y + i\lambda p_i^z) \left[ \frac{p_j^0 - p_j^x}{p_i^0 - p_i^x} \right]^{1/2} - (p_j^y + i\lambda p_j^z) \left[ \frac{p_i^0 - p_i^x}{p_j^0 - p_j^x} \right]^{1/2} \right) \quad (14a)$$

and satisfy

$$\text{(a)} \qquad \mathrm{SM}(\lambda, p_i, p_j) = -\mathrm{SM}(-\lambda, p_i, p_j)^*,$$

$$\text{(b)} \qquad \mathrm{SM}(\lambda, p_i, p_j) = -\mathrm{SM}(\lambda, p_j, p_i),$$

$$\text{(b')} \qquad \mathrm{SM}(\lambda, p_i, p_i) = 0. \quad (14b)$$

(ii) If one of the four-vectors is $k_0$, then

$$\text{(a)} \qquad \mathrm{SM}(\lambda, p_i, k_0) = -\mathrm{SM}(\lambda, k_0, p_i) = \eta_i,$$

$$\text{(a')} \qquad \mathrm{SM}(\lambda, k_0, k_0) = 0. \quad (14c)$$

Finally, we have to choose a suitable expression for the polarization four-vector of the photon. To deal with massive spinors, an adequate choice is the generalization of the one defined in ref. [5] for the massless case to the one given by

$$\varepsilon^\mu(k, \lambda) = N \bar{u}(k, \lambda) \gamma^\mu u(p, \lambda), \quad (15)$$

where $u(p, \lambda)$ is a massive spinor, $p$ any four-momenta (here taken as $p_1$) and $N$ is the normalization factor given by

$$N = \left( \sqrt{2 |\mathrm{SM}(\lambda, k, p)|^2} \right)^{-1}. \quad (16)$$

It is straightforward to see that this polarization vector satisfies the relations

$$k_\mu \varepsilon^\mu(k, \lambda) = \varepsilon_\mu(k, \lambda) \varepsilon^\mu(k, \lambda) = 0, \qquad \varepsilon_\mu(k, \lambda) \varepsilon^\mu(k, -\lambda) = -1,$$

$$\varepsilon_\mu(k, -\lambda) = \varepsilon_\mu^*(k, \lambda). \quad (17)$$

With the use of eqs. (10) and (15) we can express the amplitude $T_1(p_i, \lambda_i)$ as a function of the $Z(p_i, \lambda_i)$ functions like

$$T_1(p_1, \lambda_1; p_2, \lambda_2; k, \lambda_k; p_3, \lambda_3; p_4, \lambda_4)$$

$$= N \sum_{\lambda} (Z(p_3, \lambda_3, p_1, \lambda, p_2, \lambda_2, p_4, \lambda_4) Z(p_1, \lambda, p_1, \lambda_1, k, \lambda_k, p_1, \lambda_3)$$

$$- Z(p_3, \lambda_3, k, \lambda, p_2, \lambda_2, p_4, \lambda_4) Z(p_3, \lambda, p_1, \lambda_1, k, \lambda_k, p_1, \lambda_3)), \quad (18)$$

which are easily calculated for a particular helicity configuration once we have generated an event according to a phase space distribution. In appendix A we work in detail the expression of $Z(p_i, \lambda_i)$ for a given helicity configuration as function of the quantities $\mathrm{SM}(\lambda, q_i, q_j)$ and give a list of the $Z(p_i, \lambda_i)$ functions for all possible configurations.

As stated before, all other amplitudes can be obtained from $iM_1$ by adequate permutations and conjugations. Then, the general procedure consists on adding all the amplitudes for a given helicity configuration, multiply by the complex conjugated and sum over all possible helicity configurations. Since particles are massive, chiral projectors are not helicity projectors and therefore all amplitudes are different from zero. Nevertheless, since the $t$ channel is obviously dominant and $m_f/E \ll 1$, only the amplitudes corresponding to chirality conservation for the $t$ channel in the case of massless particles, i.e.

$$++\lambda++ \qquad +-\lambda+- \qquad -+\lambda-+ \qquad --\lambda-- \quad (19)$$

contribute significantly to the matrix element. Moreover, as we will see in the next section, the contribution of the $Z^0$ boson to the matrix element is small. Therefore, for an approximated estimation one can consider only eight photonic amplitudes and speed up considerably the calculations.

## 3. The phase space

For an efficient generation of events, we have made a detailed study of the phase space in order to find the adequate approximants which smooth the behaviour of the matrix element. Since we are interested in tagging on the photon and antitagging on the final state fermions, we express the phase space as function of the polar angle of the photon ($\vartheta_\gamma$) and outgoing fermion ($\vartheta_f$) with respect to the incident positron, the energy of the photon ($E_\gamma$) and the two trivial azimuthal angles ($\phi_\gamma$ and $\phi_f$).

Then, a single photon event is defined specifying the limits of integration of these variables. That is, if we call $\vartheta_v$ the veto angle for the final state fermions, $\vartheta_d$ the tagging angle for photons and $x_{k_{min}}$ the minimum fraction of energy for the photon with respect to the beam energy, a single photon event is defined as:

$$\begin{aligned}
&\text{(i)} && -1 \leqslant \cos\vartheta_f \leqslant -\cos\vartheta_v\,, \qquad \cos\vartheta_v \leqslant \cos\vartheta_f \leqslant 1\,,\\
&\text{(ii)} && x_{k_{min}} \leqslant x_k \leqslant x_{k_{max}}\,,\\
&\text{(iii)} && -\cos\vartheta_d \leqslant \cos\vartheta_k \leqslant \cos\vartheta_d\,,\\
&\text{(iv)} && 0 \leqslant \phi_f \leqslant 2\pi\,,\\
&\text{(v)} && 0 \leqslant \phi_k \leqslant 2\pi\,,
\end{aligned} \tag{20}$$

where $x_{k_{max}}$ is the maximum fraction of energy kinematically allowed for the photon.

With these variables, the phase space can be expressed as

$$\mathrm{d}^5\Gamma = W_{PS}\,\mathrm{d}x_k\,\mathrm{d}\Omega_k\,\mathrm{d}\Omega_{p_3}\,, \tag{21a}$$

where

$$W_{PS} = \tfrac{1}{8}E_b^2\frac{x_k\beta_{p_3}^2 x_{p_3}}{2\beta_{p_3} + x_k(\cos\vartheta_{kp_3} - \beta_{p_3})}\,, \tag{21b}$$

$$x_i = \frac{E_i}{E_b}\,, \qquad \beta_{p_3} = \frac{|\boldsymbol{P}_{p_3}|}{E_{p_3}}\,, \tag{21c}$$

$$\mathrm{d}\Omega_i = \mathrm{d}(\cos\vartheta_i)\,\mathrm{d}\phi_i\,. \tag{21d}$$

In the case where the mass of the particles can be neglected, $W_{PS}$ takes the simpler form

$$W_{PS} \cong \tfrac{1}{16}E_b^2\frac{x_k x_{p_3}^2}{1 - x_k}\,, \tag{22}$$

which will be used to construct the approximant of the cross section.

The different amplitudes corresponding to the Feynman diagrams shown in fig. 1 have a fermion propagator and a photon propagator. Since we are interested in hard photon emission, the fermion propagator can peak only in the case where the photon tends to be collinear with the fermion but, due to the tag on the photon and

antitag on the fermions, this configuration is not allowed by momentum conservation. We can therefore assume that the fermion propagator does not represent an important problem. The situation is quite different for the photonic propagator. The $s$-channel is harmless since the invariant mass of the initial or final state leptons is high. On the contrary, the $t$-channel can give a huge peak when a final state fermion tends to be collinear with the incident one. This is the peak we have to study in detail in order to find an appropriate approximant so that we can use an importance sampling algorithm for the numeric integration and generation of events.

In general, the matrix element corresponding to the diagrams of fig. 1 can be written (keeping only the relevant masses for our configuration) as

$$|\overline{M}_T|^2 = A_0 + \frac{A_1}{(p_2k)(p_4k)t} + \frac{A'_1}{(p_1k)(p_3k)t'}, \tag{23}$$

where the $A_i$ have a smooth behaviour (since do not depend on $t^{-1}$ or $t'^{-1}$) and $A_1$ and $A'_1$ are symmetric under the exchange of particle for antiparticle. Due to the kinematics, the final state leptons cannot be simultaneously collinear with the incident particles. Therefore, the peaks of the photonic propagator in $t$ and $t'$ do not occur simultaneously and we can use the superposition principle to obtain an approximant based on the simple independent functions $\sigma_{app}$ given by

$$d^5\sigma_{app} \propto \frac{1}{(p_2k)(p_4k)t} \frac{x_k x_{p_3}^2}{(1-x_k)} \, dx_k \, d\Omega_k \, d\Omega_{p_3}, \tag{24}$$

and $\sigma'_{app}$ obtained from $\sigma_{app}$ by the exchange of particle for antiparticle. Due to the symmetry of the problem it is enough then to study $\sigma_{app}$. If we define

$$\rho = \sqrt{1 + \frac{m^2}{E_b^2}}, \qquad \delta = \frac{m^2}{E_b^2} \frac{\left(1 - \max(x_{p_3})\right)^2}{2\max(x_{p_3})^2}, \tag{25}$$

we can express the approximant for the cross section (see appendix A for a detailed description) as

$$d\sigma_{app} = \frac{d\xi}{\delta + \xi} \frac{dx_k}{x_k} \frac{d\cos\vartheta_k}{(\rho - \cos\vartheta_k)^2} d\phi_{p_3} \, d\phi_k = \prod_{i=0}^{4} \kappa_i \, d\eta_i \tag{26}$$

being $\xi = 1 + \cos\vartheta_{p_3}$, $\eta_i \in [0,1]$ the new variables of integration used to absorb the

peaks in the differential cross section given by

$$\eta_0 = \begin{cases} \kappa_0^{-1} \ln \dfrac{(\delta+\xi)(\delta+1-\cos\vartheta_v)}{\delta(\delta+1+\cos\vartheta_v)}, & \cos\vartheta_{p_3} > \cos\vartheta_v \\ \kappa_0^{-1} \ln \dfrac{\delta+\xi}{\delta}, & \cos\vartheta_{p_3} < -\cos\vartheta_v \end{cases},$$

$$\eta_1 = \kappa_1^{-1} \ln \frac{x_k}{x_{k_{\min}}},$$

$$\eta_2 = \kappa_2^{-1} \left( \frac{1}{\rho - \cos\vartheta_k} - \frac{1}{\rho + \cos\vartheta_d} \right),$$

$$\eta_3 = \kappa_3^{-1} \phi_{p_3},$$

$$\eta_4 = \kappa_4^{-1} \phi_k, \tag{27}$$

and the $\kappa_i$ are the normalization constants given by

$$\kappa_0 = \ln \frac{(\delta+2)(\delta+1-\cos\vartheta_v)}{\delta(\delta+1+\cos\vartheta_v)},$$

$$\kappa_1 = \ln \frac{x_{k_{\max}}}{x_{k_{\min}}},$$

$$\kappa_2 = \frac{2\cos\vartheta_d}{\rho^2 - \cos^2\vartheta_d},$$

$$\kappa_3 = \kappa_4 = 2\pi. \tag{28}$$

The inverse transformations, necessary for the integration of the cross section and generation of events are given by

$$\xi = \begin{cases} -\delta + \delta \left( \dfrac{(\delta+2)(\delta+1-\cos\vartheta_v)}{\delta(\delta+1+\cos\vartheta_v)} \right)^{\eta_0}, & \eta_0 < \eta_{\lim} \\ -\delta + \delta \left( \dfrac{\delta+1+\cos\vartheta_v}{\delta+1-\cos\vartheta_v} \right) \left( \dfrac{(\delta+2)(\delta+1-\cos\vartheta_v)}{\delta(\delta+1+\cos\vartheta_v)} \right)^{\eta_0}, & \eta_0 > \eta_{\lim} \end{cases},$$

$$x_k = x_{k_{\min}} \left( \frac{x_{k_{\max}}}{x_{k_{\min}}} \right)^{\eta_1},$$

$$\cos\vartheta_k = \rho - \frac{\rho^2 - \cos^2\vartheta_d}{\rho - (1-2\eta_2)\cos\vartheta_d},$$

$$\phi_{p_3} = 2\pi\eta_3, \qquad \phi_k = 2\pi\eta_4, \tag{29}$$

being

$$\eta_{\lim} = \ln \frac{\delta + 1 - \cos \vartheta_v}{\delta} \Big/ \ln \frac{(\delta + 2)(\delta + 1 - \cos \vartheta_v)}{\delta(\delta + 1 + \cos \vartheta_v)} . \tag{30}$$

Since all variables are then independent, we can write

$$\sigma_{app} = \int_{1+\cos\vartheta_v}^{2} \int_0^{1-\cos\vartheta_v} \frac{d\xi}{\delta+\xi} \int_{x_{k_{min}}}^{x_{k_{max}}} \frac{dx_k}{x_k} \int_{-\cos\vartheta_d}^{\cos\vartheta_d} \frac{d\cos\vartheta_k}{(\rho - \cos\vartheta_k)^2} \int_0^{2\pi} d\phi_{p_3} \int_0^{2\pi} d\phi_k$$

$$= \prod_{i=0}^{4} \kappa_i \int_0^1 d\eta_i = \prod_{i=0}^{4} \kappa_i . \tag{31}$$

The existing symmetry between $\sigma_{app}$ and $\sigma'_{app}$ leads to the same value of the integral and the same distributions when the kinematic variables are transformed as

$$E_{p_3} \Leftrightarrow E_{p_4} ,$$

$$\boldsymbol{p}_3 \Leftrightarrow -\boldsymbol{p}_4 ,$$

$$\boldsymbol{k} \Leftrightarrow -\boldsymbol{k} . \tag{32}$$

If we take the variables $\eta_i$ uniformly distributed in $[0,1]$ we obtain, by means of the transformations (29), the variables of the phase space distributed in such a way that they reproduce the important peaks of the differential cross section. Then, the total cross section will be given by

$$\sigma_T = \int_\Omega |M_T|^2 \, d^5\Gamma$$

$$= \int_\Omega \frac{|M_T|^2}{|M_{app}|^2 + |M'_{app}|^2} \left( |M_{app}|^2 + |M'_{app}|^2 \right) d^5\Gamma$$

$$= \int_\Omega \frac{|M_T|^2}{|M_{app}|^2 + |M'_{app}|^2} \left( d\sigma_{app} + d\sigma'_{app} \right)$$

$$= \left\langle \frac{|M|^2_T}{|M_{app}|^2 + |M'_{app}|^2} \right\rangle_{(app, app')} \cdot \left( \sigma_{app} + \sigma'_{app} \right) . \tag{33}$$

Therefore

$$\sigma_T = 2\left( \langle WT \rangle \pm \Delta_{\langle WT \rangle} \right) \sigma_{app} , \tag{34a}$$

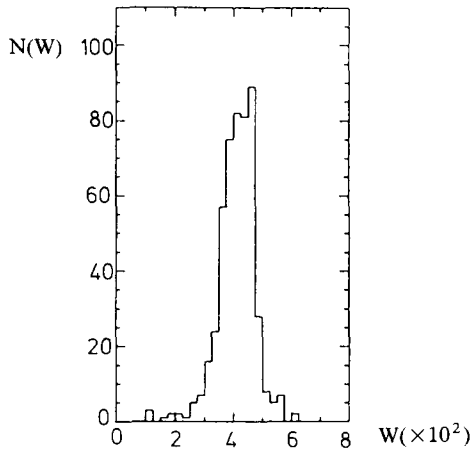


Fig. 2. Distribution of event weights.

where

$$\mathrm{WT} = \left\langle \frac{|M|_{\mathrm{T}}^2}{|M_{\mathrm{app}}|^2 + |M'_{\mathrm{app}}|^2} \right\rangle_{(\mathrm{app},\mathrm{app}')} \tag{34b}$$

has to be calculated generating 50% of the events with $\mathrm{d}^5\sigma_{\mathrm{app}}$ and 50% with $\mathrm{d}^5\sigma'_{\mathrm{app}}$ since the value of the integrals is the same. Due to the existing symmetry between both approximants, the most efficient way would be to generate the events with $\mathrm{d}^5\sigma_{\mathrm{app}}$ (or $\mathrm{d}^5\sigma'_{\mathrm{app}}$) and apply the transformation (32) to 50% of them. In order to obtain the events according to the probability given by the cross section, we have to apply a rejection algorithm to the weight WT to correct for the approximated distribution. In the present case and for the cuts specified in sect. 4, the distribution of weights obtained by sampling 1000 events is shown in fig. 2. The small variance of the distribution shows that the mapping we have used in order to absorb the peaking structure of the matrix element squared is very efficient. For the practical generation of events, the use of an adaptative stratified sampling algorithm allows us to obtain a more refined approximation to the cross section in such a way that the variance of the estimation of the integral is reduced and the generation efficiency increased.

## 4. Results

In this section we will discuss some relevant distributions of the process $e^+e^- \to e^+e^-\gamma$ together with* $e^+e^- \to \nu\bar{\nu}\gamma$ for a c.m. energy of $\sqrt{s} = 100$ GeV with $M_{Z^0} = 93$

* Using a similar procedure, we have calculated the complete $g^3$ order contribution to $e^+e^- \to \nu\bar{\nu}\gamma$ and found very good agreement with the approximated cross section obtained by Gaemers et al. (see ref. [1]).

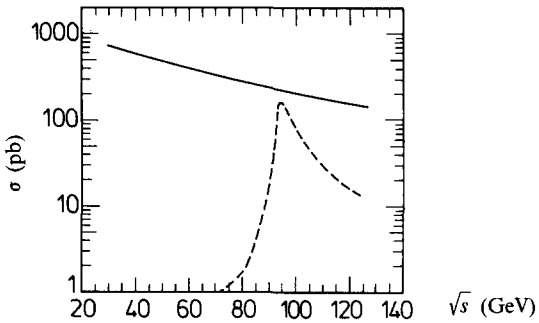


Fig. 3. Cross section as function of $\sqrt{s}$ for $e^+e^- \to e^+e^-\gamma$ (solid line) and $e^+e^- \to \nu\bar{\nu}\gamma$ (dashed line).

GeV, $\sin^2\vartheta_w = 0.22$ and a hypothetical experimental set-up defined by

(i) veto angle for electrons of $\vartheta_v = 5°$,

(ii) tagging angle for photons of $\vartheta_d = 20°$, and

(iii) minimum photon energy* of 1 GeV.

The cross section for the processes $e^+e^- \to e^+e^-\gamma$ and $e^+e^- \to \nu\bar{\nu}\gamma$ under the experimental conditions previously referred is shown in fig. 3. As one can see, the big cross section for the radiative Bhabha scattering (solid line) decreases with $\sqrt{s}$. For the particular selection cuts the photonic $t$-channel is by far the most relevant, being the effect of the $Z^0$ boson negligible. We have superimposed the cross section for $e^+e^- \to \nu\bar{\nu}\gamma$ (dashed line). In this case, since the $s$-channel with the $Z^0$ is dominant, there is a clear peak when the center of mass energy is close to the $Z^0$ resonance.

The differential cross section as function of the photon energy for the processes $e^+e^- \to e^+e^-\gamma$ and $e^+e^- \to \nu\bar{\nu}\gamma$ is shown in fig. 4. Again, there is no significant effect due to the $Z^0$ boson for $e^+e^- \to e^+e^-\gamma$ (continuous histogram) while in the case of $e^+e^- \to \nu\bar{\nu}\gamma$ (dotted histogram) there is a peak when

$$E_\gamma = \frac{s - M_{Z^0}^2}{2\sqrt{s}} \qquad (\approx 6.8 \text{ GeV in this case}). \tag{35}$$

This may allow a study of the process $e^+e^- \to \nu\bar{\nu}\gamma$ performing a subtraction of the background from $e^+e^- \to e^+e^-\gamma$ for energies such that in the region where the photon energy is peaked there is a reasonable signal-to-noise ratio.

For an efficient reduction of the contamination from $e^+e^- \to e^+e^-\gamma$, the photon transverse momentum ($P\!\!\!/$) distribution is more relevant. The differential cross section as function of $P\!\!\!/$ for the two processes is shown in fig. 5. Due to the tagging conditions, the transverse momentum for the photon in the process $e^+e^- \to e^+e^-\gamma$

* For a very small value of $x_{k\,\min}$ ($x_{k\,\min} < 0.001$) it is necessary to include higher order electromagnetic corrections which, if necessary, can be estimated by exponentiation of the leading log terms.

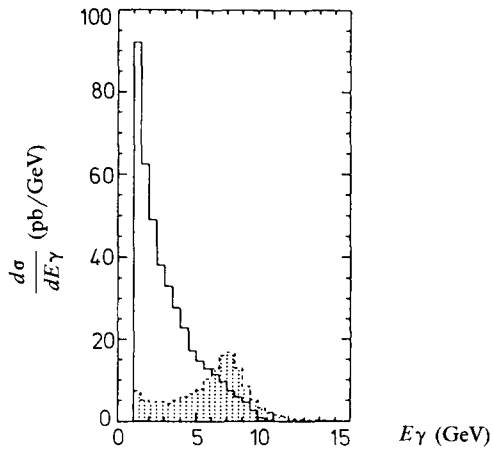


Fig. 4. Differential cross section as function of the photon energy for $e^+e^- \to e^+e^-\gamma$ (continuous histogram) and $e^+e^- \to \nu\bar{\nu}\gamma$ (dotted histogram).

is limited by

$$P^{\gamma}_{T,\max} = \frac{\sqrt{s}\sin\vartheta_v}{1+\sin\vartheta_v} \qquad (\approx 8.7 \text{ GeV in this case}). \tag{36}$$

The scatter plot of $P^{\gamma}_{T}$ versus $\cos\vartheta_\gamma$ for both processes can be seen in fig. 6. One can clearly see that an adequate cut in $P^{\gamma}_{T}$ eliminates the contribution of $e^+e^- \to e^+e^-\gamma$ and leaves a significant signal for $e^+e^- \to \nu\bar{\nu}\gamma$ in the central part of the detector (fig. 7).

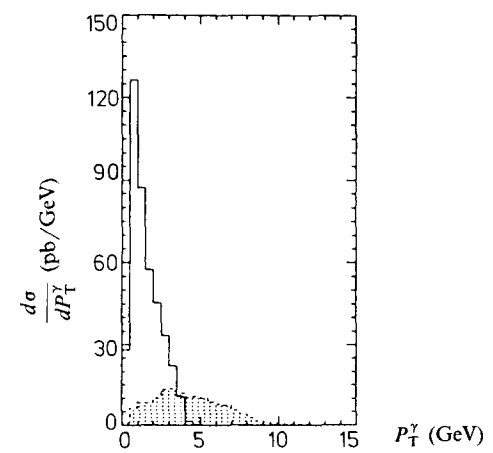


Fig. 5. Differential cross section as function of the photon transverse momentum for the same processes and specifications as before.

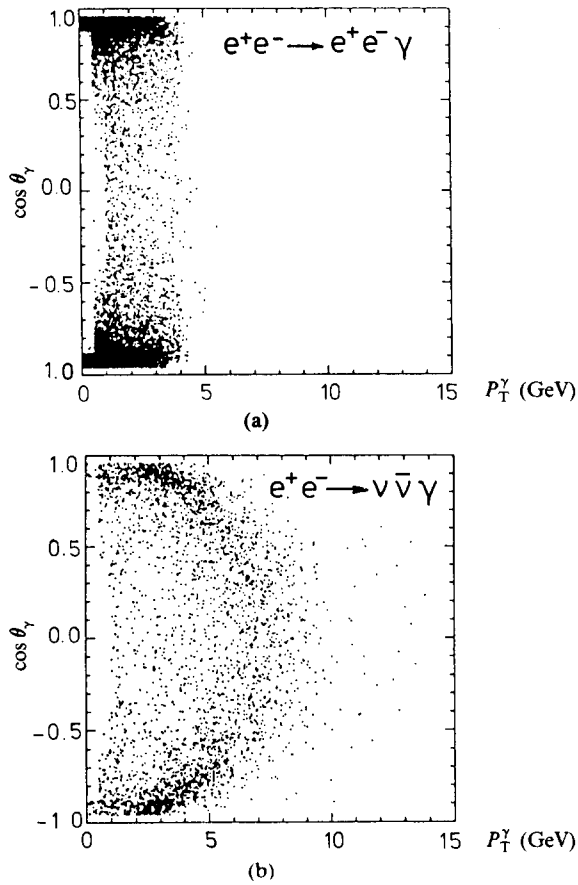


Fig. 6. Scatter plot of the transverse momentum of the photon versus $\cos\vartheta_\gamma$ for $e^+e^- \to e^+e^-\gamma$ (fig. 6a) and $e^+e^- \to \nu\bar{\nu}\gamma$ (fig. 6b) the number of entries in both plots is normalized to the relative cross sections.

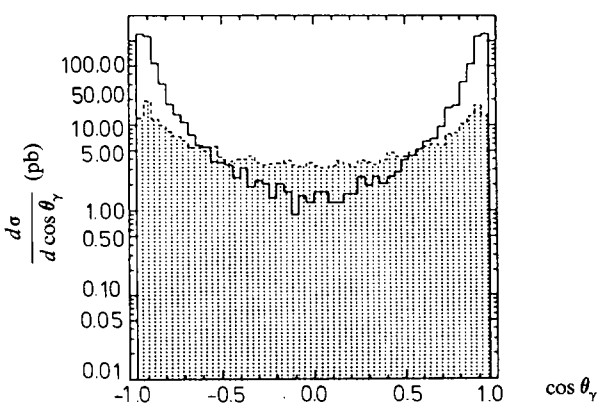


Fig. 7. Distribution of $\cos\vartheta_\gamma$ for $e^+e^- \to e^+e^-\gamma$ (continuous histogram) and $e^+e^- \to \nu\bar{\nu}\gamma$ (dotted histogram).

## 5. Comparison with other calculations

We have compared our matrix element to the one given in ref. [8] by computing its value in a region of the phase space where the fermion masses can be neglected and found perfect agreement. Nevertheless, one has to be aware of the fact that, since the fermion masses are not included in their calculation for the particular configuration we are dealing with, their result cannot be directly extrapolated to the present situation.

In a more direct comparison with some of the previous estimates of the process $e^+e^- \to e^+e^-\gamma$ as background for single $\gamma$ events, we found in particular that the results quoted in ref. [9] are wrong since they do not integrate over the region of small angles for outgoing fermions which gives a huge contribution.

Last, we have compared our calculation with the one in ref. [10] and found agreement after correcting for the fact that they use $\alpha_{em} = 1/128.5$ whereas we use $\alpha_{em} = 1/137$.

## 6. Conclusions

We have done an exact calculation of the process $e^+e^- \to e^+e^-\gamma$ to order $g^3$ and an unweighted Monte Carlo generator of events including the $\gamma$ and the $Z^0$ intermediate vector bosons and keeping fermion masses. These conditions allow us to study the contribution of this process as a background to single photon events; in particular $e^+e^- \to \nu\bar{\nu}\gamma$ which we have also calculated completely to order $g^3$. Compared to previous calculations of this background, the fact that we have done the calculation with the helicity amplitudes technique has shown to be very useful as far as simplicity and numerical stability concerns. In particular we have seen that, as obviously expected, only the eight helicity amplitudes of the photonic $t$ channel corresponding to chirality conservation for massless particles are relevant for this analysis.

Finally, we have seen that to study the process $e^+e^- \to \nu\bar{\nu}\gamma$, although it may be possible, in the region where the photon energy is peaked and the signal-to-noise ratio reasonable, to perform a background subtraction, it is in general much more efficient to make a cut in the transverse momentum of the photon because this eliminates completely the contribution of $e^+e^- \to e^+e^-\gamma$ and leaves a significant signal of $e^+e^- \to \nu\bar{\nu}\gamma$ in the central part of the detector.

## Appendix A

In this appendix we are going to show as an example, how to calculate, for a particular helicity configuration, the $Z(p_i, \lambda_i)$ and afterwards, give a list with all possible occurring cases so that the evaluation of any amplitude $T(p_i, \lambda_i)$ will become a trivial (but lengthy) operation easily implementable in a computer program.

As we have seen in sect. 3, the $Z(p_i, \lambda_i)$ functions are defined as

$$Z(p_i, \lambda_i; p_j, \lambda_j; p_k, \lambda_k; p_l, \lambda_l) \equiv \left[\bar{u}(p_i, \lambda_i)\Gamma^\mu u(p_j, \lambda_j)\right] \times \left[\bar{u}(p_k, \lambda_k)\Gamma'_\mu u(p_l, \lambda_l)\right]. \quad \text{(A.1)}$$

For simplicity, we will consider the case where $\Gamma^\mu = \Gamma'^\mu = \gamma^\mu$. When the function $Z(p_1, \lambda_1; p_2, \lambda_2; p_3, \lambda_3; p_4, \lambda_4)$ is expressed in terms of the chiral spinors $w(p_i, \lambda_i)$, it reads

$$\begin{aligned} &Z(p_1, \lambda_1; p_2, \lambda_2; p_3, \lambda_3; p_4, \lambda_4) \\ &\quad = \left[\bar{w}(p_1, \lambda_1) + \mu_1 \bar{w}(k_0, -\lambda_1)\right]\gamma^\mu\left[\bar{w}(p_2, \lambda_2) + \mu_2 \bar{w}(k_0, -\lambda_2)\right] \\ &\qquad \times \left[\bar{w}(p_3, \lambda_3) + \mu_3 \bar{w}(k_0, -\lambda_3)\right]\gamma_\mu\left[\bar{w}(p_4, \lambda_4) + \mu_4 \bar{w}(k_0, -\lambda_4)\right], \end{aligned} \quad \text{(A.2)}$$

which gives in general 16 terms of the form $F^\mu(\lambda_i, q_i, q_j)F_\mu(\lambda_k, q_k, q_l)$. As an example, consider the case where $\lambda_1 = \lambda_2 = \lambda_3 = \lambda_4 = +$. Then, since

$$\bar{w}(p_i, +)\gamma^\mu w(k_0, -) = \bar{w}(k_0, -)\gamma^\mu w(p_i, +) = 0 \quad \text{(A.3)}$$

the expression reduces to

$$\begin{aligned} Z(++++) &= \left[\bar{w}(p_1, +)\gamma^\mu w(p_2, +) + \mu_2\mu_1 \bar{w}(k_0, -)\gamma^\mu w(k_0, -)\right] \\ &\quad \times \left[\bar{w}(p_3, +)\gamma_\mu w(p_4, +) + \mu_3\mu_4 \bar{w}(k_0, -)\gamma_\mu w(k_0, -)\right] \\ &= \left[f^\mu(+, p_1, p_2) - \mu_1\mu_2 f_\mu(+, k_0, k_0)\right] \\ &\quad \times \left[f_\mu(+, p_3, p_4) - \mu_3\mu_4 f_\mu(+, k_0, k_0)\right] \end{aligned} \quad \text{(A.4)}$$

after having used the relation (12). Then, using eqs. (13) and (14), we can express

this product as function of the quantities $\mathrm{SM}(\lambda, p_i, p_j)$. In this case we have

$$\begin{aligned}
&\text{(i)} \quad f^\mu(+, p_1, p_2) f_\mu(+, p_3, p_4) = -2\,\mathrm{SM}(+, p_1, p_3)\mathrm{SM}(-, p_2, p_4),\\
&\text{(ii)} \quad f^\mu(+, p_1, p_2) f_\mu(+, k_0, k_0) = -2\,\mathrm{SM}(+, p_1, k_0)\mathrm{SM}(+, p_2, k_0)\\
&\qquad\qquad = -2\eta_1\eta_2,\\
&\text{(iii)} \quad f^\mu(+, k_0, k_0) f_\mu(+, p_3, p_4) = -2\,\mathrm{SM}(+, k_0, p_4)\mathrm{SM}(+, k_0, p_3)\\
&\qquad\qquad = -2\eta_3\eta_4,\\
&\text{(iv)} \quad f^\mu(+, k_0, k_0) f_\mu(+, k_0, k_0) = 0. \qquad\qquad \text{(A.5)}
\end{aligned}$$

Therefore

$$\begin{aligned}
Z(p_1, +, p_2, +, p_3, +, p_4, +) = &-2\,\mathrm{SM}(+, p_1, p_3)\mathrm{SM}(-, p_2, p_4)\\
&+2\mu_1\mu_2\eta_3\eta_4 + 2\eta_1\eta_2\mu_3\mu_4. \qquad\qquad \text{(A.6)}
\end{aligned}$$

To obtain the expression of the functions $Z(p_i, \lambda_i)$ we have written a program in algebraic language (REDUCE) which allows us to handle expressions of $\Gamma^\mu$ more complicated than the ones we are dealing with (eq. (2.1)). In particular, for the case where $\Gamma^\mu = \gamma^\mu(C_\mathrm{L}P_\mathrm{L} + C_\mathrm{R}P_\mathrm{R})$ we found, in agreement with ref. [6] (besides a trivial misprint) that*

$$\begin{aligned}
Z(+,+,+,+) &= -2(\mathrm{SM}(+, p_3, p_1)\mathrm{SM}(-, p_4, p_2)C'_\mathrm{R}C_\mathrm{R}\\
&\qquad -\mu_1\mu_2\eta_3\eta_4 C'_\mathrm{R}C_\mathrm{L} - \eta_1\eta_2\mu_3\mu_4 C'_\mathrm{L}C_\mathrm{R}),\\
Z(+,+,+,-) &= -2\eta_2 C_\mathrm{R}(\mathrm{SM}(+, p_4, p_1)\mu_3 C'_\mathrm{L} - \mathrm{SM}(+, p_3, p_1)\mu_4 C'_\mathrm{R}),\\
Z(+,+,-,+) &= -2\eta_1 C_\mathrm{R}(\mathrm{SM}(-, p_2, p_3)\mu_4 C'_\mathrm{L} - \mathrm{SM}(-, p_2, p_4)\mu_3 C'_\mathrm{R}),\\
Z(+,+,+,+) &= -2(\mathrm{SM}(+, p_3, p_1)\mathrm{SM}(-, p_4, p_2)C'_\mathrm{R}C_\mathrm{R}\\
&\qquad -\mu_1\mu_2\eta_3\eta_4 C'_\mathrm{R}C_\mathrm{L} - \eta_1\eta_2\mu_3\mu_4 C'_\mathrm{L}C_\mathrm{R}),\\
Z(+,-,+,+) &= -2\eta_4 C'_\mathrm{R}(\mathrm{SM}(+, p_3, p_1)\mu_2 C_\mathrm{R} - \mathrm{SM}(+, p_3, p_2)\mu_1 C_\mathrm{L}),\\
Z(+,-,+,-) &= +0,\\
Z(+,-,-,+) &= -2(\mu_1\mu_4\eta_2\eta_3 C'_\mathrm{L}C_\mathrm{L} + \mu_2\mu_3\eta_1\eta_4 C'_\mathrm{R}C_\mathrm{R} - \mu_2\mu_4\eta_1\eta_3 C'_\mathrm{L}C_\mathrm{R}\\
&\qquad -\mu_1\mu_3\eta_2\eta_4 C'_\mathrm{R}C_\mathrm{L}),\\
Z(+,-,-,-) &= -2\eta_3 C'_\mathrm{L}(\mathrm{SM}(+, p_2, p_4)\mu_1 C_\mathrm{L} - \mathrm{SM}(+, p_1, p_4)\mu_2 C_\mathrm{R}). \qquad \text{(A.7)}
\end{aligned}$$

* Note that for $\Gamma^\mu = \gamma^\mu$ one just has to set $C_\mathrm{L} = C_\mathrm{R} = 1$.

Due to the existing symmetry, one can obtain the remaining configurations interchanging all the helicity indices, that is, $\mathrm{SM}(\lambda, p_i, p_j) \leftrightarrow \mathrm{SM}(-\lambda, p_i, p_j)$ and $L \leftrightarrow R$.

## Appendix B

As explained in sect. 3, in order to have an efficient numeric integration of the cross section, we have absorbed the peaking structures of the photonic $t$ channel in an approximated differential cross section which is afterwards corrected applying the appropriate weights. Since the peaking structures in $|M_T|^2$ are of the form $t^{-1}$ (or $t'^{-1}$) we can construct an approximant as

$$\mathrm{d}^5\sigma_{\mathrm{app}} \propto \frac{1}{(p_2k)(p_4k)t}\,\frac{x_k x_{p_3}^2}{(1-x_k)}\,\mathrm{d}x_k\,\mathrm{d}\Omega_k\,\mathrm{d}\Omega_{p_3}, \tag{B.1}$$

and similarly for $\sigma'_{\mathrm{app}}$ interchanging particle for antiparticle. Taking the $Z$ axis as $\boldsymbol{U}_{e^+}$, we have that

$$\begin{aligned} t &= -2E_b^2 x_{p_3}\left(\delta + 1 + \cos\vartheta_{p_3}\right), \\ (p_2k) &= E_b^2 x_k(\rho - \cos\vartheta_k), \\ (p_4k) &= E_b^2 \frac{x_k x_{p_3}}{1-x_k}\left(\rho + \cos\vartheta_{kp_3}\right), \end{aligned} \tag{B.2}$$

where we have defined

$$\rho = \sqrt{1 + \frac{m^2}{E_b^2}}, \qquad \delta = \frac{E_b^2 x_{p_3} - |\boldsymbol{P}_1|\,|\boldsymbol{P}_3| - m^2}{|\boldsymbol{P}_1|\,|\boldsymbol{P}_3|} \tag{B.3}$$

and used explicitly the relation

$$x_{p_3} = \frac{2(1-x_k)}{2 - x_k + x_k\cos\vartheta_{kp_3}} \tag{B.4}$$

due to energy-momentum conservation. Therefore, we can write the expression (24) as

$$\mathrm{d}\sigma_{\mathrm{app}} = \frac{\mathrm{d}x_k\,\mathrm{d}\cos\vartheta_k\,\mathrm{d}\cos\vartheta_{p_3}\,\mathrm{d}\phi_k\,\mathrm{d}\phi_{p_3}}{x_k(\rho - \cos\vartheta_k)\left(\delta + 1 + \cos\vartheta_{p_3}\right)\left(\rho + \cos\vartheta_{kp_3}\right)}. \tag{B.5}$$

The term $\cos\vartheta_{kp_3}$ correlates $\vartheta_k$ and $\vartheta_{p_3}$ but, due to the kinematics of the problem, is obvious that it is dominated by $\vartheta_k$ since the direction of the outgoing electron is very close to the beam direction. Therefore, we can eliminate all correlations among the variables considering

$$\cos\vartheta_{kp_3} \sim -\cos\vartheta_k$$

and write

$$d\sigma_{app} = \frac{d\cos\vartheta_{p_3}}{\delta + 1 + \cos\vartheta_{p_3}} \frac{dx_k}{x_k} \frac{d\cos\vartheta_k}{(\rho - \cos\vartheta_k)^2} d\phi_{p_3} d\phi_k = \prod_{i=0}^{4} \kappa_i \, d\eta_i , \qquad (B.6)$$

where $\eta_i \in [0,1]$ and $\kappa_i$ are the corresponding normalization factors. Since we expect $\cos\vartheta_{p_3} \sim -1$ we will use, for numerical accuracy, the variable $\xi = 1 + \cos\vartheta_{p_3}$. Last, since in our case $E^2 \gg m^2$ we can make a Taylor expansion of the modulus of the trimomenta appearing in the numerator of the function $\delta$ defined in (B.3). Keeping terms of order $O(m^2)$ we have that

$$|\boldsymbol{P}_1| \, |\boldsymbol{P}_3| \cong E_{p_1} E_{p_3} \left( 1 - \tfrac{1}{2} m^2 \frac{E_{p_1}^2 + E_{p_3}^2}{E_{p_1}^2 E_{p_3}^2} \right). \qquad (B.7)$$

Therefore

$$\delta \cong \frac{m^2}{2E_{p_1}E_{p_3}} \frac{E_{p_1}^2 + E_{p_3}^2 - 2E_{p_1}E_{p_3}}{E_{p_1}E_{p_3}} = \frac{m^2}{E_b^2} \frac{(1 - x_{p_3})^2}{2x_{p_3}^2} . \qquad (B.8)$$

As we see, $\delta$ depends on $x_{p_3}$. Nevertheless, since $x_{p_3}$ will be very peaked to the maximum value kinematically allowed (so the momentum transfer is minimum), we can fix it to this value and neglect any variation. This gives the approximant we used in eq. (26) of sect. 3.

We want to thank F. Cornet and S. Rodriguez for a careful reading of the paper, R. Gatto and M. Caffo for interesting discussions and some of the members of the MARK-J Collaboration, in particular B. Zhou and H.G. Wu., for their help in checking the event generator. We are also indebted to the DESY directory for their hospitality.

## References

[1] E. Ma and J. Okada, Phys. Rev. Lett. 41 (1978) 287
K.J.F. Gaemers, R. Gastmans and R.M. Renard, Phys. Rev. D19 (1979) 1605
[2] P. Fayet, Phys. Lett. 117B (1982) 460;
J. Ellis and J. Hagelin, Phys. Lett. 122B (1982) 303;
M. Martinez, PhD thesis, Barcelona Univ. (1986)
[3] F.A. Berends and R. Kleiss, Nucl. Phys. B228 (1983) 537
[4] P. de Causmaker et al. (CALKUL Collaboration), Nucl. Phys. B206 (1982) 53;
G.R. Ferrar and F. Neri, Phys. Lett. 130B (1983) 109;
F.A. Berends et al. (CALKUL Collaboration), DESY 83-125 report (1983)
[5] Z. Xu, Da-Hua Zhang and Lee Chang, Tsinghua Univ. report TUTP 84/3 (1984);
R. Kleiss and W.J. Stirling, Nucl. Phys. B262 (1985) 235
[6] P.H. Daverveldt, PhD thesis, Leiden Univ. (1985)
[7] F.A. Berends, P.H. Daverveldt and R. Kleiss, Nucl. Phys. B253 (1985) 441
[8] F.A. Berends et al., Nucl. Phys. B206 (1982) 61
[9] E. Simopolou, CERN 86-02 report (1986) p. 197
[10] M. Caffo, R. Gatto and E. Remiddi, DFUB 86/5 report (1986)